

Voltage stability assessment using PMUs and STATCOM

Suresh Babu Palepu, Manubolu Damodar Reddy

Department of Electrical and Electronics Engineering, Sri Venkateswara University College of Engineering, Tirupati, India

Article Info

Article history:

Received May 6, 2022

Revised Nov 11, 2022

Accepted Nov 29, 2022

Keywords:

Nose curves

PMU

STATCOM

Voltage stability

VSM

ABSTRACT

Since the previous few decades, researchers and utilities have been extremely concerned about voltage instability because to the numerous instances of system blackouts caused by voltage instability that have been recorded in various regions of the world. With the development of synchro phasor technology, it appears conceivable to track and manage the system's voltage stability in real time. This study suggests using phasor measuring units (PMUs) placed strategically to monitor voltage stability margin online and to regulate it using a static synchronous compensator (STATCOM). According to the minimum reactive and real power loanability for the most of the line outages, STATCOM has been installed at the critical bus. Based on the difference between the bus voltage and its reference value, STATCOM supplies reactive power into the bus. PMU measurements are used to determine bus voltages at regular intervals, and reactive power is then added to the bus online as necessary. The increased voltage stability margin brought on by STATCOM injecting reactive power is continuously checked. Based on simulations performed on the IEEE 14-bus system and the New England 39-bus system, the effectiveness of the suggested approach for online monitoring and management of voltage stability margin (VSM) has been proven.

This is an open access article under the [CC BY-SA](https://creativecommons.org/licenses/by-sa/4.0/) license.



Corresponding Author:

Suresh Babu Palepu

Department of Electrical and Electronics Engineering

Sri Venkateswara University College of Engineering, Tirupati, India

Email: sureshram48@gmail.com

1. INTRODUCTION

Voltage stability maintenance is crucial for the safe operation of power systems. Voltage instability may cause unacceptable low voltages to develop in a sizable portion of the network, which could cause voltage collapse in a sizable area [1]. The system has been advised to use a number of control strategies to guard against voltage breakdown. Lack of reactive support is one of the main causes of voltage instability. Reactive power transmission is challenging, especially under pressure. Local reactive support at essential buses therefore appears to be a workable solution to voltage instability. The advent of flexible AC transmission system (FACTS) controllers, which can efficiently control voltage stability of the system, is the result of advancements in power electronics technology [2]. A shunt controller called static synchronous compensator (STATCOM), which is a member of the FACTS family, can increase the voltage stability margin by injecting reactive power into the bus. Given the high cost, it's crucial to deploy STATCOM at the best position. Voltage stability margin is typically improved by providing adequate reactive power assistance at the crucial bus or weakest bus of the system. For the placement of STATCOM, the L-index based technique to identify key buses has been taken into consideration [3], [4]. Since Tokyo's voltage collapse, the P-V and Q-V curves based approach has been frequently utilized to determine the best position and size for STATCOM [5], [6]. These methods demand a lot of time and space.

The position and size of FACTS devices have been determined using a variety of heuristic methods. The ideal size and location of FACTS devices have been determined using mixed integer linear and non-linear programming. Local minima and computing effort provide a challenge, albeit [7]–[11]. The STATCOM size and allocation problem can be resolved using the evolutionary computation method known as particle swarm optimization (PSO). Numerous power system concerns, including economic load dispatch, generating gaps, and short-term load forecasts, have benefited from the application of this technique. For the best location and size of STATCOM to increase load ability and voltage stability, a Particle Swarm Optimization-based technique and other related techniques are reported [12]–[20]. To increase the voltage stability of the power system network, Lei and Fei suggested an innovative nonlinear (IN) H-control for STATCOM [21]. The IN H-control for STATCOM in this study was designed using the Hamiltonian function technique. The idea of trajectory sensitivity is used to identify important buses in a suggested systematic strategy for improving short-term voltage stability [22]. It has been suggested that STATCOM should control power directly depending on the transit of active power as a result of injecting or absorbing reactive power [23].

The majority of studies on STATCOM's involvement in improving the voltage stability of offline systems have been taken into consideration. It appears that voltage stability of online systems can be monitored and managed with the development of phasor measurement units (PMUs) [24]. This study suggests employing phasor measurement units to monitor and regulate the voltage stability of online systems used with STATCOM. Given that STATCOM placement is an offline strategy, the system's crucial bus, as determined by the continuation power flow (CPF) method [25], has been appropriately located herein. However, it has been suggested for the online systems to monitor and adjust the voltage stability margin due to the reactive power injection by STATCOM to the crucial bus utilizing bus voltages monitored by phasor measuring units at regular intervals.

2. STATCOM PLACEMENT STRATEGY

As an offline technique, STATCOM placement is chosen based on the maximum load ability determined by the continuation power flow (CPF) approach. The peak reactive power and peak real power load ability at every bus are determined for the intact system scenario and all single line outage instances. Reactive power and real power demand were varied in accordance with the following to achieve peak reactive power load ability and real power load ability:

$$P_{D_i} = P_{D_{ib}}(1 + \lambda_{ip}) \quad (1)$$

$$Q_{D_i} = Q_{D_{ib}}(1 + \lambda_{iq}) \quad (2)$$

Were: P_{D_i} = Real power demand at bus- i ; Q_{D_i} = Reactive power demand at bus- i ; $P_{D_{ib}}$ = Real power demand at bus- i at the base case operating point ; $Q_{D_{ib}}$ = Reactive power demand at bus- i at the base case operating point; λ_{ip} = Fraction of real power demand increase at bus- i ; λ_{iq} = Fraction of reactive power demand increase at bus- i .

For the majority of contingency instances, STATCOM is situated on the bus with the lowest real power load ability and reactive power load ability. This work takes into account the STATCOM voltage regulator model shown in Figure 1, which supplies reactive power into the bus based on how much the bus voltage deviates from its reference value, subject to a maximum and minimum injection current limit (viz. i_{max} and i_{min} as shown).

Dynamic model of STATCOM state equation is given by,

$$i_{SH} = (K_r(V_{ref} - V_k) - i_{SH})/T_r \quad (3)$$

Were: i_{SH} = Current injected to bus by STATCOM; V_{ref} = Reference value of bus voltage magnitude; V_k = Voltage of bus- k (the bus where STATCOM is placed); K_r = Gain of voltage regulator; T_r = Time constant of voltage regulator. Reactive power (Q_{SH}) injected by STATCOM is given by,

$$Q_{SH} = i_{SH}V \quad (4)$$

as injected current and bus voltage are taken to be in phase quadrature.

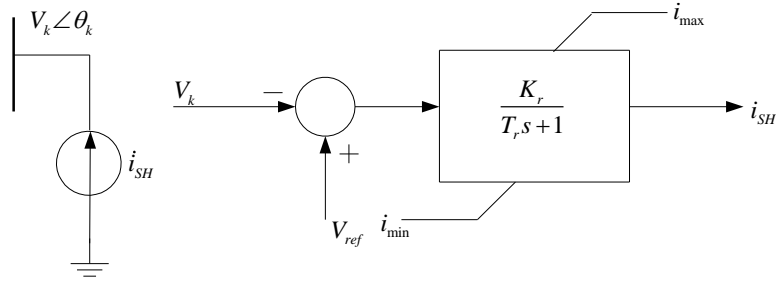


Figure 1. STATCOM model

3. METHODOLOGY FOR ON-LINE CONTROL OF VOLTAGE STABILITY MARGIN THROUGH STATCOM

Pseudo measurements and phasor measurements unit (PMU) measurements carried out at three operational conditions are used to monitor the voltage stability margin of the system used with STATCOM online. Fresh PMU measurements are carried out and updated voltage stability information is obtained at frequent intervals because operating points are constantly changing as a result of changes in operating conditions and network topology. Based on the outcomes of binary spider monkey algorithm approach for optimal siting of phasor measurement unit for power system state estimation [26], PMUs are strategically positioned in the network to ensure complete network observability even in the event of PMU failure.

To calculate the magnitude of the voltage across all the buses, pseudo measurements and phasor measurements unit (PMU) measurements carried out at the 3 operating conditions. The bus's reactive power injection by STATCOM at the 3 operating conditions are calculated in accordance with (3) and (4). By quadratic fitting of nose curves based on pseudo measurements and PMU measurements collected at 3 operating conditions as follows, the voltage stability margin (peak reactive power load ability as well as real power load ability) of the network used with STATCOM is derived:

Voltage magnitude V_i versus real power demand (P_{D_i}) curve of bus- i shown in Figure 2 may be roughly acquired by solution of quadratic equation as shown in (5).

$$P_{D_i} = a_{1i}V_i^2 + a_{2i}V_i + a_{3i} \quad (5)$$

Where, a_{1i} , a_{2i} and a_{3i} are constants. Differentiating P_{D_i} with respect to V_i ,

$$\frac{dP_{D_i}}{dV_i} = 2a_{1i}V_i + a_{2i} \quad (6)$$

P - V curve at nose point, $\frac{dP_{D_i}}{dV_i} = 0$. Consequently, from (6)

$$V_i^{np} = -\frac{a_{2i}}{2a_{1i}} \quad (7)$$

where, V_i^{np} = bus- i voltage magnitude at the P - V curve's peak shown in Figure 2. In (5) and (7)

$$P_{D_i}^n = -\frac{a_{2i}^2}{4a_{1i}} + a_{3i} \quad (8)$$

where $P_{D_i}^n$ = At the peak of the P - V curve, the real power requirement of bus- i shown in Figure 2.

By solving a quadratic equation, the reactive power demand versus voltage magnitude curve (Q - V curve) of bus- i shown in Figure 3 can be roughly determined.

$$Q_{D_i} = b_{1i}V_i^2 + b_{2i}V_i + b_{3i} \quad (9)$$

where, b_{1i} , b_{2i} and b_{3i} are constants. Differentiating Q_{D_i} with respect to V_i

$$\frac{dQ_{D_i}}{dV_i} = 2b_{1i}V_i + b_{2i} \quad (10)$$

At the nose point of Q - V curve, $\frac{dQ_{D_i}}{dV_i} = 0$, Therefore, from (10)

$$V_i^{nq} = -\frac{b_{2i}}{2b_{1i}} \quad (11)$$

where, V_i^{nq} = bus- i voltage magnitude at the Q - V curve's peak shown in Figure 3. From (9) and (11)

$$Q_{D_i}^n = -\frac{b_{2i}}{4b_{1i}} + b_{3i} \quad (12)$$

where $Q_{D_i}^n$ = Bus- i reactive power requirement at the Q - V curve's peak shown in Figure 3.

Equations are solved to obtain constants a_{1i} , a_{2i} and a_{3i} :

$$P_{D_i}^1 = a_{1i}(V_i^1)^2 + a_{2i}V_i^1 + a_{3i} \quad (13)$$

$$P_{D_i}^2 = a_{1i}(V_i^2)^2 + a_{2i}V_i^2 + a_{3i} \quad (14)$$

$$P_{D_i}^3 = a_{1i}(V_i^3)^2 + a_{2i}V_i^3 + a_{3i} \quad (15)$$

where, V_i^1 , V_i^2 , V_i^3 shown in Figure 3 and in Figure 2 measure the magnitude of voltage of bus- i at 3, 2 and 1, operating points respectively, and $P_{D_i}^3$, $P_{D_i}^2$ and $P_{D_i}^1$ shown in Figure 2 related to real power demand of bus- i at 3, 2 and 1, operating points correspondingly.

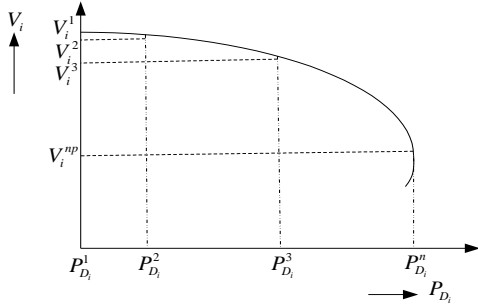


Figure 2. P - V curve of bus- i

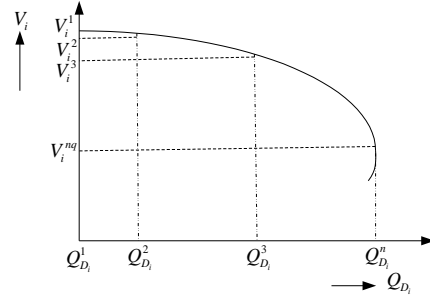


Figure 3. Q - V curve of bus- i

Calculated constants a_{1i} , a_{2i} and a_{3i} are used to determine maximum real power loading of bus- i using (8). Constants b_{1i} , b_{2i} and b_{3i} are calculated by solutions of equations:

$$Q_{D_i}^1 = b_{1i}(V_i^1)^2 + b_{2i}V_i^1 + b_{3i} \quad (16)$$

$$Q_{D_i}^2 = b_{1i}(V_i^2)^2 + b_{2i}V_i^2 + b_{3i} \quad (17)$$

$$Q_{D_i}^3 = b_{1i}(V_i^3)^2 + b_{2i}V_i^3 + b_{3i} \quad (18)$$

where, $Q_{D_i}^3$, $Q_{D_i}^2$ and $Q_{D_i}^1$ shown in Figure 3 related to reactive power demand of bus- i at 3, 2 and 1, operating points correspondingly. Determined constants b_{1i} , b_{2i} and b_{3i} are used to calculate maximum reactive power load ability of bus- i considering (12).

The real power demand, reactive power demand and voltage magnitude acquired from pseudo measurements/PMU measurements carried out at operating points 3, 2, and 1 are used to evaluate constants, b_{1i} , b_{2i} , b_{3i} a_{1i} , a_{2i} and a_{3i} for every load bus. Peak reactive power load ability and maximum real power load ability of every bus are predicted by evaluated constants using (8) and (12), respectively. Peak real power load ability of the system is defined as the least out of peak real power load ability of every load bus present in the system, and the corresponding bus is regarded as the most important bus based on peak real power load ability. According to the peak reactive power load ability criterion, the corresponding bus is regarded as the most crucial bus because it has the lowest peak reactive power load ability of all the load buses that are present in the system. Figure 4 depicts the flow chart for online monitoring of the voltage stability margin and its control using STATCOM. Since the peak load ability of a real-time system changes as operating conditions change, it is suggested to update the maximum load ability as well as the bus

information that is most important to the system on a regular basis using new PMU measurements. The flowchart in Figure 4 starts off with high maximum initial load abilities of 10,000 MVAR and 10,000 MW, respectively, keeping in mind that these values are higher than the maximum load abilities of any of the load buses in the system. It then gradually reduces these values until the most critical bus has reached its maximum reactive power and real power load abilities. STATCOM injects reactive power in accordance with (3) and (4) after each PMU measurement (4).

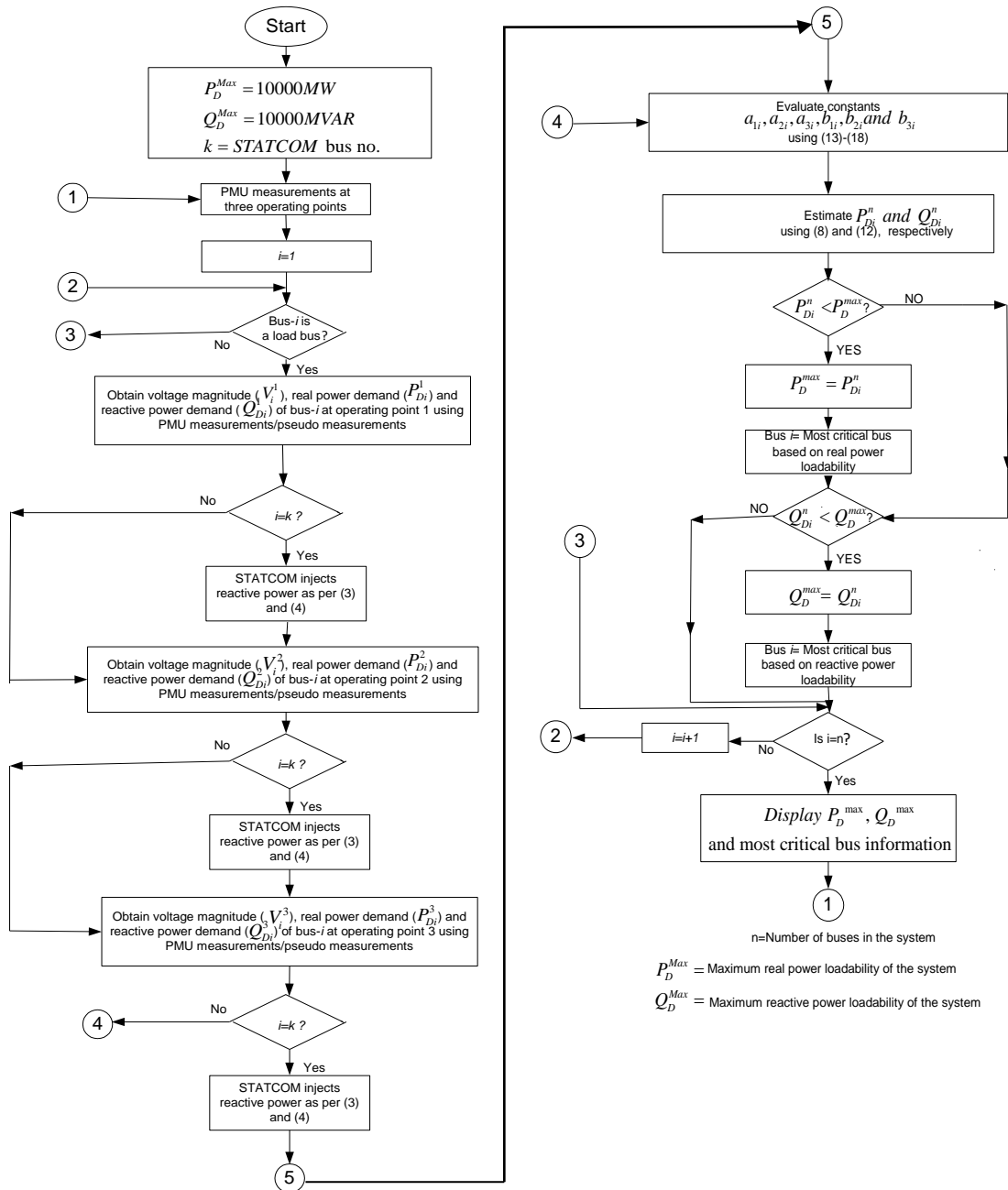


Figure 4. Flowchart for online control of maximum load ability using STATCOM

4. RESULTS AND DISCUSSION

Case studies were performed on IEEE 14-bus system and a New England 39-bus system. Below are reported the results of two systems' simulations:

4.1. IEEE-14 bus system [27]

IEEE-14 bus system consists of three synchronous condensers (at 8, 6, 3 bus numbers), two synchronous generators (at 2, 1 bus numbers), three synchronous condensers (at bus numbers 3, 6, 8), and 20 transmission lines (including 3 transformers). Continuation power flows were run to determine peak real power load ability as well as peak reactive power load ability of each bus for the system intact case and all the single line failure cases. For running continuation power flows, reactive and real power demand at each bus was varied as per (1) and (2), respectively. Maximum real power load ability (P_D^{Max}) along with critical bus number based on real power load ability, have been shown in Table 1 for the intact system case and few critical contingency cases. Maximum reactive power load ability (Q_D^{Max}) along with critical bus number based on reactive power load ability, have been shown in Table 2 for the intact system case and few critical contingency cases. It is observed from Table 1 and Table 2 that bus-5 is the most critical bus based on real power load ability as well as reactive power load ability for majority of critical contingencies. Therefore, bus-5 was selected as the optimal location for the placement of STATCOM.

Based on the outcomes of Binary spider monkey algorithm approach for optimal siting of phasor measurement unit for power system state estimation, PMUs were installed at buses 2, 4, 5, 6, and 9 to ensure complete system observability even in the event of PMU failure of a few. Using the flowchart in Figure 4, the maximum reactive and real power load ability of the system with STATCOM installed at bus-5 was computed for both the system intact case and all single line failure instances. Based on the flowchart shown in Figure 4 and disregarding the blocks corresponding to STATCOM, real and reactive power load ability for the system without STATCOM were also calculated in order to validate the adequacy of the STATCOM deployment strategy.

Table 1. Critical bus real power load ability under critical contingencies was achieved using the CPF approach

C.C.	Intact case	1-2	2-3	2-4	1-5	2-5
P_D^{Max} (MW)	40.20	16.19	30.11	32.91	34.50	35.26
C.B.	5	5	4	5	5	5

Table 2. Critical bus reactive power load ability under critical contingencies was achieved using the CPF approach

C.C.	Intact case	1-2	2-3	9-14	6-13	9-10
Q_D^{Max} (MVAR)	8.46	0.54	3.07	5.22	6.04	6.10
C.B.	5	5	4	14	13	10

C.C. = critical contingency, P_D^{Max} , Q_D^{Max} = maximum active and reactive power load ability, C.B. = critical bus

The continuous power flow (CPF) method was used to determine the real and reactive power load ability for systems with and without STATCOM. For the intact system case and a few key contingency cases, the real and reactive power load ability of the system with and without STATCOM have been demonstrated in Table 3 and Table 4, respectively. The placement of STATCOM at the ideal location (i.e., bus number 5) leads to a notable improvement in the voltage stability margin, as can be seen from Table 3 and Table 4. Figure 5 compares the nose curves of important bus 5 during the line outage 2-3 using real power collected using the suggested approach with and without STATCOM. The nose curves of crucial bus 5 computed using the suggested technique without and with STATCOM for the line failure 2-3 employing reactive power are also shown in Figure 6. Figure 5 and Figure 6 show that placing STATCOM at bus 5 significantly increases the voltage stability margin.

4.2. New England 39-bus system [28]

The New-England 39-bus system has 46 transmission lines and ten generators with twelve zero-injection buses at bus numbers 1, 2, 6, 5, 9, 10, 13, 11, 14, 19, 17 and 22. New England 39-bus system for the intact system scenario and all single line failure cases, continuation power flows were used to calculate the peak reactive power load ability and peak real power load ability of every bus. Real and reactive power demands at each bus were adjusted in accordance with (1) and (2), respectively, for running continuation power flows. For the intact system scenario and a few important contingency cases, the peak real power load ability and critical bus number based on real power load ability are shown in Table 5. Table 6 for the intact system case and a few important contingency cases displays the peak reactive power load ability as well as the critical bus number based on reactive power load ability. Based on real power load ability and reactive power load ability for the majority of key scenarios.

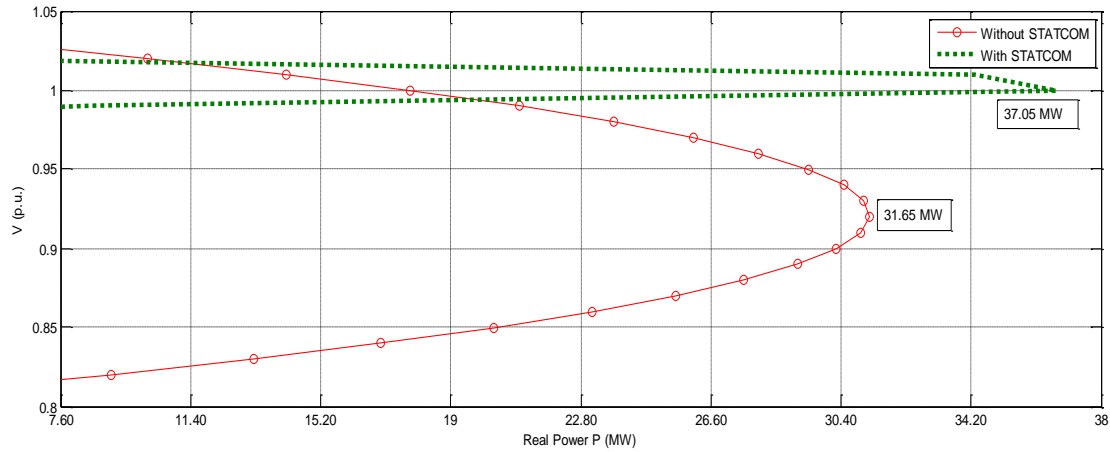


Figure 5. Comparison of P - V curves of critical bus 5 without STATCOM and with STATCOM for line failure 3-2 based on PMU measurements

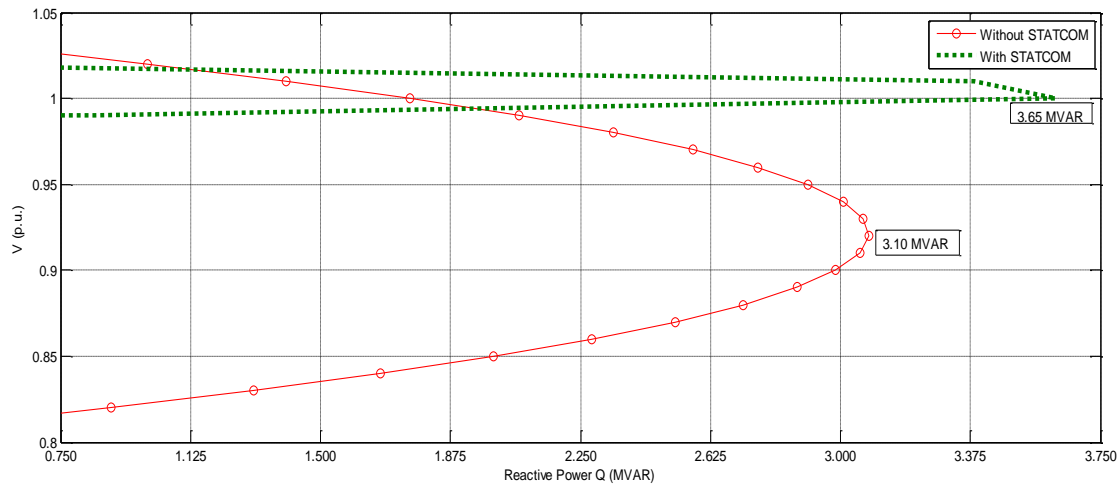


Figure 6. Comparison of Q - V curves of critical bus 5 without STATCOM and with STATCOM for line failure 3-2 based on PMU measurements

Table 3. Real power load ability of the system with and without STATCOM

Critical contingency	PMU measurements		CPF method	
	Without STATCOM P_b^{Max} (MW)	With STATCOM at bus- 5 P_b^{Max} (MW)	Without STATCOM P_b^{Max} (MW)	With STATCOM at bus- 5 $5P_b^{Max}$ (MW)
Intact	39.44	49.60	40.20	43.77
1-2	17.78	20.20	16.49	17.63
2-3	31.65	37.05	30.11	33.42
2-4	32.76	43.71	32.91	38.32
1-5	37.39	40.66	34.50	39.03
2-5	35.64	42.93	35.26	44.59

Table 4. Reactive power load ability of the system with and without STATCOM

Critical contingency	PMU measurements		CPF method	
	Without STATCOM Q_b^{Max} (MVAR)	With STATCOM at bus- 5 $5Q_b^{Max}$ (MVAR)	Without STATCOM Q_b^{Max} (MVAR)	With STATCOM at bus- 5 $5Q_b^{Max}$ (MVAR)
Intact	7.81	9.25	8.46	9.05
1-2	0.56	1.27	0.54	0.58
2-3	3.10	3.65	3.07	4.73
6-13	5.57	9.08	6.04	6.38
9-14	4.68	7.31	5.22	6.44
9-10	5.64	8.30	6.10	6.50

It can be seen from Table 5 and Table 6 that bus-29 is the most critical bus. As a result, bus-29 was chosen as the ideal site for the installation of STATCOM. 21 PMUs were placed at bus numbers 4, 8, 12, 16, 18, 20, 23, 25, 26, 27, 29, 30, 31, 32, 33, 34, 35, 36, 37, 38 and 39. Based on the findings of the binary spider monkey algorithm, full network observability is guaranteed even in the event of a small PMU loss [18] by assuring the optimal siting of phasor measurement units for power system state estimation. Using the flowchart in Figure 4, the maximum real and reactive power load ability of the system considering STATCOM installed at bus number 29 was computed for both the intact system case and all single line outage instances. Real and reactive power load ability were also determined for the system without STATCOM using the been demonstrated in Table 7 and Table 8, respectively. Tables 7 and 8 show that placing STATCOM in the ideal location-bus number 29-affects the voltage stability margin significantly more. Figure 7 compares the nose curves of important bus 29 for the line failure 38-29 using the suggested technique without and with STATCOM. A comparison of the critical bus 29's nose curves computed using the suggested approach without and with STATCOM for the line failure 38-29 is also shown in Figure 8. Figure 7 and Figure 8 show that placing STATCOM at bus-29 significantly increases the voltage stability margin.

Table 5. Peak real power loadability of critical bus under critical contingencies calculated by cpf approach

C.C.	Intact case	21-22	28-29	22-35	10-32	29-38
P_D^{Max} (MW)	1686.83	930.60	989.42	1099.98	1102.82	2380
C.B.	29	23	29	29	29	20

Table 6. Peak reactive power loadability of critical bus under critical contingencies calculated by cpf approach

C.C.	Intact case	2-25	29-38	28-29	10-32	15-16
Q_D^{Max} (MVAR)	151.01	51.26	72.10	88.58	98.73	168.90
C.B.	5	5	4	14	13	10

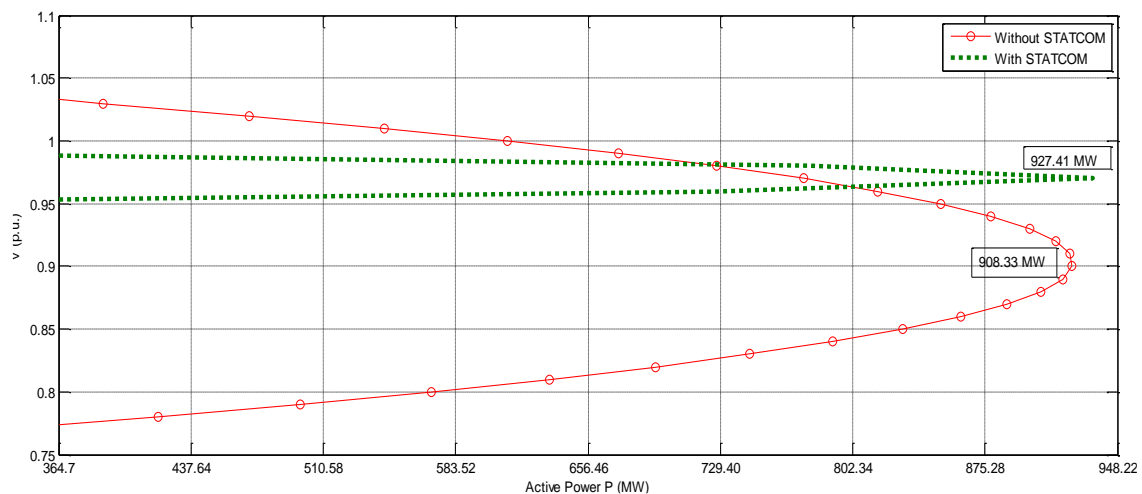


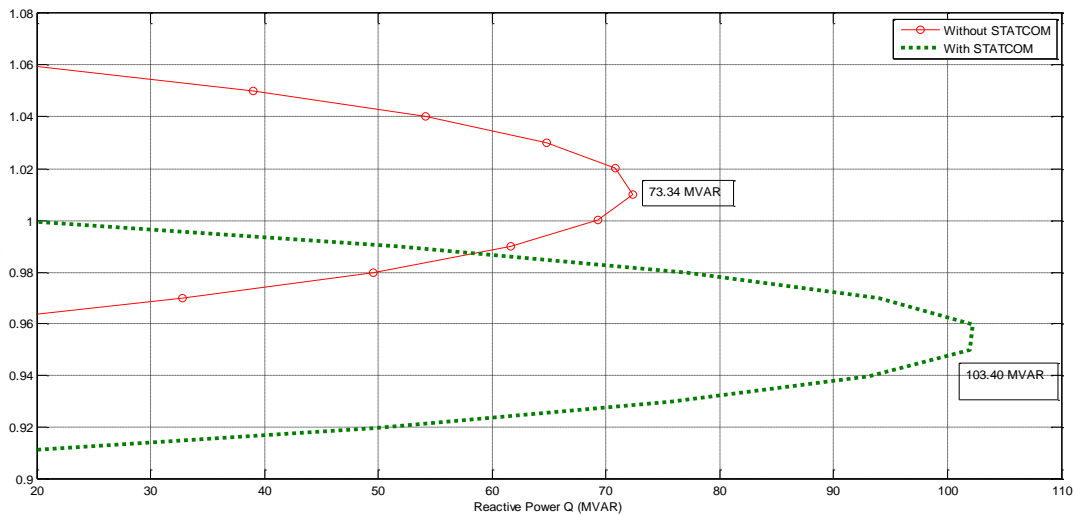
Figure 7. Comparison of P - V curves of critical bus 29 without STATCOM and with STATCOM for line outage 22-21 based on PMU measurements

Table 7. Real power load ability of the system with and without STATCOM

Critical contingency	PMU measurements		CPF method	
	Without STATCOM P_D^{Max} (MW)	With STATCOM at bus-29 P_D^{Max} (MW)	Without STATCOM P_D^{Max} (MW)	With STATCOM at bus-29 P_D^{Max} (MW)
Intact	1363.64	1419.85	1686.83	1702.68
28-29	856.17	926.73	989.42	1003.23
21-22	908.33	927.41	930.60	943.28
22-35	1108.49	1117.63	1099.98	1104.45
10-32	1114.16	1144.15	1102.82	1107.47

Table 8. Reactive power load ability of the system with and without STATCOM

Critical contingency	PMU measurements		CPF method	
	Without STATCOM Q_b^{Max} (MVAR)	With STATCOM at bus-29 Q_b^{Max} (MVAR)	Without STATCOM Q_b^{Max} (MVAR)	With STATCOM at bus-29 Q_b^{Max} (MVAR)
Intact	122.08	127.11	151.01	157.23
28-29	76.65	82.97	88.58	98.32
29-38	73.34	103.40	72.10	75.91
15-16	142.60	150.93	168.90	169.41
2-25	42.10	43.45	51.26	51.97
10-32	99.74	102.43	98.73	99.15

Figure 8. Comparison of Q - V curves of critical bus 29 without STATCOM and with STATCOM for line outage 38-29 based on PMU measurements

5. CONCLUSION

The majority of research has focused on controlling and monitoring the voltage stability of offline systems. This work proposes reactive power injection using STATCOM for real-time monitoring and control of online systems. Based on voltage measurements taken by PMUs at three successive operation points, the voltage stability margin has been measured in real time. Based on the difference between the bus voltage magnitude and its predefined value, STATCOM supplies reactive power to the crucial bus (the bus where it is installed). Using updated PMU data, the increased voltage stability margin caused by reactive power injection is checked often. The efficiency of the suggested method of real-time management of voltage stability margin through reactive power supply by STATCOM is demonstrated by case studies carried out on three test systems.




REFERENCES

- [1] B. H. Lee and K. Y. Lee, "A study on voltage collapse mechanism in electric power systems," *IEEE Transactions on Power Systems*, vol. 6, no. 3, pp. 966–974, 1991, doi: 10.1109/59.119236.
- [2] N. G. Hingoranl, L. Gyugyi, and M. E. El-Hawary, "Understanding FACTS: Concepts and technology of flexible ac transmission systems," *Understanding FACTS: Concepts and Technology of Flexible AC Transmission Systems*, pp. 1–432, 1999, doi: 10.1109/9780470546802.
- [3] P. Mishra, H. N. Udupa, and G. Piyush, "Calculation of Sensitive Node for IEEE-14 Bus System When Subjected to Various Changes in Load," *IRAJ International Conference*, 2013.
- [4] N. Sanivarapu, R. Kalaivani, and S. R. Paranjothi, "Optimal Location of STATCOM to Improve Voltage Stability using PSO," *International Journal of Advanced Engineering Technology*, vol. 2, no. 4, pp. 62–74, 2011.
- [5] C. W. Taylor, *Power System Voltage Stability*. McGraw-Hill, 1994.
- [6] P. Kundur, *Power System Stability and Control*. McGraw-Hill, 1993.
- [7] N. Yorino, E. E. El-Araby, H. Sasaki, and S. Harada, "A new formulation for FACTS allocation for security enhancement against voltage collapse," *IEEE Transactions on Power Systems*, vol. 18, no. 1, pp. 3–10, 2003, doi: 10.1109/TPWRS.2002.804921.
- [8] Z. G. Sanchez, J. A. G. C. Cruz, G. C. Sanchez, H. H. Herrera, and J. I. S. Ortega, "Voltage collapse point evaluation considering the load dependence in a power system stability problem," *International Journal of Electrical and Computer Engineering*, vol. 10, no. 1, pp. 61–71, 2020, doi: 10.11591/ijece.v10i1.pp61-71.
- [9] M. Chiranjivi and K. Swarnasri, "A novel optimization-based power quality enhancement using dynamic voltage restorer and distribution static compensator," *Indonesian Journal of Electrical Engineering and Computer Science*, vol. 6, no. 1, pp. 160–171, 2022, doi: 10.11591/ijeecs.v26.i1.pp160-171.




- [10] M. R. Zaidan and S. I. Toos, "Emergency congestion management of power systems by static synchronous series compensator," *Indonesian Journal of Electrical Engineering and Computer Science*, vol. 25, no. 3, pp. 1258–1265, 2022, doi: 10.11591/ijeecs.v25.i3.pp1258-1265.
- [11] P. S. BABU, P. B. CHENNAIAH, and M. SREEHARI, "Optimal Placement of SVC Using Fuzzy and Firefly Algorithm," *IAES International Journal of Artificial Intelligence (IJ-AI)*, vol. 4, no. 4, p. 113, 2015, doi: 10.11591/ijai.v4.i4.pp113-117.
- [12] Y. V. Krishna Reddy and M. Damodar Reddy, "Flower pollination algorithm to solve dynamic economic loading of units with piecewise fuel options," *Indonesian Journal of Electrical Engineering and Computer Science*, vol. 16, no. 1, pp. 9–16, 2019, doi: 10.11591/ijeecs.v16.i1.pp9-16.
- [13] S. B. Palepu and M. D. Reddy, "Optimal PMU Placement for Power System State Estimation Using Improved Binary Flower Pollination Algorithm," *2021 6th International Conference on Recent Trends in Electronics, Information, Communication and Technology, RTEICT 2021*, pp. 800–804, 2021, doi: 10.1109/RTEICT52294.2021.9573518.
- [14] A. V. S. Reddy, M. D. Reddy, and M. S. Kumar Reddy, "Network Reconfiguration of Primary Distribution System Using GWO Algorithm," *International Journal of Electrical and Computer Engineering (IJECE)*, vol. 7, no. 6, p. 3226, 2017, doi: 10.11591/ijece.v7i6.pp3226-3234.
- [15] R. Babu and B. Bhattacharyya, "Optimal placement of PMU for complete observability of the interconnected power network considering zero-injection bus: A numerical approach," *International Journal of Applied Power Engineering (IJAPE)*, vol. 9, no. 2, p. 135, 2020, doi: 10.11591/ijape.v9.i2.pp135-146.
- [16] M. Baba, N. B. M. Nor, T. B. Ibrahim, and M. A. Sheikh, "A comprehensive review for optimal placement of phasor measurement unit for network observability," *Indonesian Journal of Electrical Engineering and Computer Science*, vol. 19, no. 1, pp. 301–308, 2020, doi: 10.11591/ijeecs.v19.i1.pp301-308.
- [17] J. B. Park, K. S. Lee, J. R. Shin, and K. Y. Lee, "A particle swarm optimization for economic dispatch with nonsmooth cost functions," *IEEE Transactions on Power Systems*, vol. 20, no. 1, pp. 34–42, 2005, doi: 10.1109/TPWRS.2004.831275.
- [18] S. Kannan, S. M. R. Slochanal, and N. P. Padhy, "Application and comparison of metaheuristic techniques to generation expansion planning problem," *IEEE Transactions on Power Systems*, vol. 20, no. 1, pp. 466–475, 2005, doi: 10.1109/TPWRS.2004.840451.
- [19] C. M. Huang, C. J. Huang, and M. L. Wang, "A particle swarm optimization to identifying the ARMAX model for short-term load forecasting," *IEEE Transactions on Power Systems*, vol. 20, no. 2, pp. 1126–1133, 2005, doi: 10.1109/TPWRS.2005.846106.
- [20] J. Vishnu *et al.*, "A strategy for optimal loading pattern of a typical power system - A case study," *2014 International Conference on Advances in Green Energy, ICAGE 2014*, pp. 112–117, 2014, doi: 10.1109/ICAGE.2014.7050152.
- [21] B. Lei and S. Fei, "IN H ∞ control for STATCOM to improve voltage stability of power system," *Electronics Letters*, vol. 53, no. 10, pp. 670–672, May 2017, doi: 10.1049/el.2016.4617.
- [22] Y. Xu, Z. Y. Dong, K. Meng, W. F. Yao, R. Zhang, and K. P. Wong, "Multi-objective dynamic VAR planning against short-term voltage instability using a decomposition-based evolutionary algorithm," *IEEE Transactions on Power Systems*, vol. 29, no. 6, pp. 2813–2822, 2014, doi: 10.1109/TPWRS.2014.2310733.
- [23] K. I. Sayahi, A. Kadri, R. Karwi, and F. Bacha, "Study and implementation of a static compensator (STATCOM) using direct power control strategy," *2018 9th International Renewable Energy Congress, IREC 2018*, pp. 1–6, 2018, doi: 10.1109/IREC.2018.8362508.
- [24] P. Sahu and M. K. Verma, "On-line voltage stability monitoring and control in smart grid - A survey," *2015 IEEE UP Section Conference on Electrical Computer and Electronics, UPCON 2015*, 2016, doi: 10.1109/UPCON.2015.7456714.
- [25] V. Ajjarapu and C. Christy, "The continuation power flow: A tool for steady state voltage stability analysis," *IEEE Transactions on Power Systems*, vol. 7, no. 1, pp. 416–423, 1992, doi: 10.1109/59.141737.
- [26] S. B. Palepu and M. D. Reddy, "Binary spider monkey algorithm approach for optimal siting of the phasor measurement for power system state estimation," *IAES International Journal of Artificial Intelligence*, vol. 11, no. 3, pp. 1033–1040, 2022, doi: 10.11591/ijai.v11.i3.pp1033-1040.
- [27] "IEEE14-Bus System." http://www.ee.washington.edu/research/pstca/pf14/pg_tca14bus.htm.
- [28] "New England 39-Bus System," [Online]. Available: <http://icseg.iti.illinois.edu/ieee-39-bus-system/>.

BIOGRAPHIES OF AUTHORS



Suresh Babu Palepu    received his B.Tech degree in Electrical and Electronics Engineering from Annamacharya Institute of Technology and sciences, Rajampet, Andhra Pradesh, India in 2006 and M.Tech degree in Power Systems from Sri Venkateswara University College of Engineering, Tirupati, and Andhra Pradesh, India in 2010. He is currently pursuing for Ph.D degree in Electrical Engineering at Sri Venkateswara University College of Engineering, Tirupati, and Andhra Pradesh, India. His research interests include capacitor, DG Placement and reconfiguration of distribution system, voltage stability studies, wide area monitoring system and smart grid. He can be contacted at email: sureshram48@gmail.com.



Manubolu Damodar Reddy    has 28 years of experience in teaching in Post Graduate level and 23 years of experience in Research. He has received M.Tech and Ph.D in Electrical Engineering from S. V. University College of Engineering, Tirupati, India, 1992 and 2008 respectively. He has a Life Member of ISTE. Presently he is working as a Professor in Electrical Engineering at S.V. University, Tirupati, India. He has published 1 Australian Patent, 63 Research (International Journals-48, International Conferences-32) Papers. Presently guiding 6 Ph.D. Scholars and 5 students are awarded. His Research area is Power system optimization and reactive power compensation. He can be contacted at email: mdreddy999@rediffmail.com.